

# FROM NON-HOLONOMIC CONSTRAINT EQUATION TO EXACT TRANSPORT ALGORITHM FOR ROLLING CONTACT

Friedrich BÖHM

Department of Mechanics  
Technical University of Berlin  
D-10587 Berlin, Germany

Received: November 2, 1994

## Abstract

The one-point contact problem roughly describing the rolling behaviour of wheels and the sliding behaviour of sleds was defined by Hertz, Cartheodory, Hamel and others. Extending this idea to a continuous field of contact points in a closed 2-dimensional domain produces the nonstationary field of tractrices in the contact area. One has to solve nonlinear partial first order differential equations or integral equations. Discretisation of the whole wheel in dynamic contact gives rise to a new method which is not based on finite element method. Measurements and computations of rolling wheels on a glass plate show that high frequency behaviour of the contact of wheels has to be taken into account to understand all phenomenas.

*Keywords:* non-holonomic constraints, transport equations, friction, stability, rough contact.

## 1. Introduction

The one-point contact problem roughly describing the rolling behaviour of wheels and the sliding behaviour of sleds was first solved by Hertz, later on by Caratheodory, Hamel, Neimark and Fuvaev and others. The analytical expression for a pure rolling condition is shown in *Fig. 1* and because of the fact that the angle  $\alpha$  for rolling must be zero there exists a differential condition  $e_n \cdot ds = 0$  or

$$-\sin \psi dx_1 + \cos \psi dy_1 + 0d\psi + 0dt = 0$$

and a rolling condition:

$$dx_1 \cos \psi + dy_1 \sin \psi = R d\varphi,$$

with the components to be seen from *Fig. 1*.

$$\frac{dx_1}{dt} = \dot{x}_1 = v_{\text{Roll}} \cos \psi, \quad \frac{dy_1}{dt} = \dot{y}_1 = v_{\text{Roll}} \sin \psi,$$

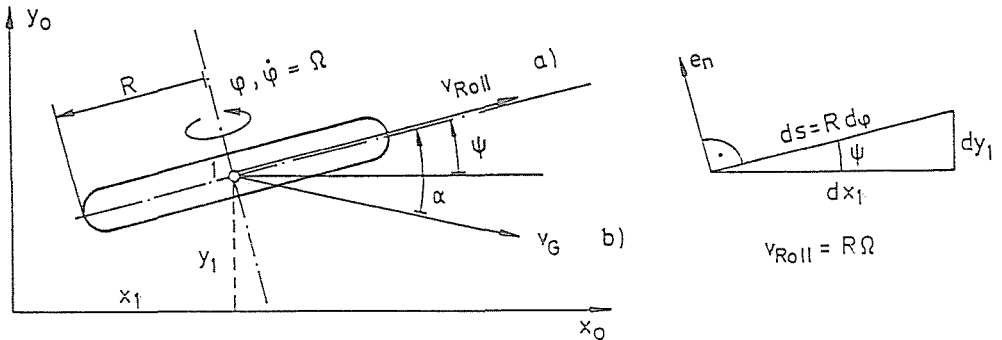


Fig. 1. Rolling wheel: fixed plane  $x_0, y_0$ , contact point  $x_1, y_1$ , sliding velocity  $v_G$ , rolling velocity  $v_{Roll}$ , radius of wheel  $R$ , angular velocity  $\Omega$ , increments of moving  $dx_1, dy_1, e_n$ , unit vector of wheel axle, direction of wheel plane  $\psi$ , non-holonomic condition is  $\alpha = 0$  and  $v_G = v_{Roll}$

which is a 'Pfaff's' form. The heading angle  $\psi$  is a free parameter and must not be chosen continuously in time. The two differentials  $dx_1$  and  $dy_1$  cannot be integrated because of the fact that the factors  $-\sin \psi$  and  $\cos \psi$  should hold the

condition

 of integrability:

$$df = \frac{\partial f}{\partial x_1} dx_1 + \frac{\partial f}{\partial y_1} dy_1 + \frac{\partial f}{\partial \psi} d\psi + \frac{\partial f}{\partial t} dt \dots \quad \text{if} \quad \boxed{\frac{\partial^2 f}{\partial x_i \partial x_j} = \frac{\partial^2 f}{\partial x_j \partial x_i}}$$

which obviously they do not (therefore it is called non-holonomic constrained condition). In analytical mechanics it was shown by Appel, Pfaff and Routh that such a condition can be used together with the equations of Newton. In the case of a skater-shoe which belongs to the same condition we get, see in Fig. 2, the following acceleration vector for the center of gravity:

$$\begin{aligned} a_x &= \dot{v}_x - \omega v_y - \omega^2 a, \\ a_y &= \dot{v}_y - \omega v_x - \dot{\omega} a. \end{aligned}$$

After some manipulations, see Appendix 1, we find the following condition for the heading angle  $\psi$ :  $\dot{\psi} = \omega$ ,

$$\dot{\omega} + \lambda \omega = 0, \quad \lambda = \frac{m a v_x}{J_s + m a^2}.$$

For the starting conditions that the velocity  $v_x$  and  $\dot{\psi}$  are also constant, the parameter  $a$  shows that there are two solutions possible. One solution is stable the other one unstable. If the center of gravity is in front of the

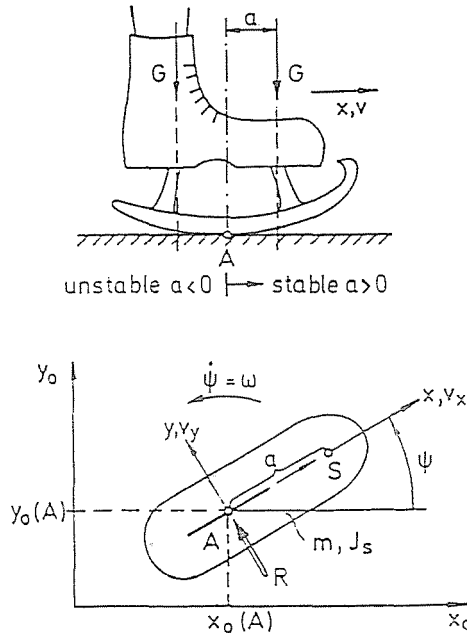


Fig. 2. Ice-skating shoe: moving plane  $x, y$ , contact point  $A$ , weight of skater  $G$ , distance to C.G ( $=S$ ) is a non-holonomic condition  $v_y = 0$ .

contact point the solution is stable. Otherwise the solution is unstable. In this case the motion of the system produces also singular points where the center of gravity is rotating around the contact point which is fixed a moment in the contact plane. From this behaviour one can conclude that every vehicle equipped with laterally not stiff front wheels and stiff rear wheels is stable (understeering).

In reality wheels show a small amount of deformation when rolling forces laterally or longitudinally occur. In Fig. 3 the lateral force is produced by a constant deformation  $\bar{y}$  and linear increasing deformation of the profile elements along the contact length of a deformable wheel. B. v. SCHLIPPE and R. DIETRICH and also RIEKERT have shown that at the front of the contact area a non-holonomic rolling condition can be defined with a heading angle  $\psi$  relative to the plane of the wheel. Using the assumption that the deformation laterally of the leading point of contact is proportional to the created lateral force and it is also proportional to the heading angle  $\psi$  we get the so-called 'relaxation length'  $L$  which marks a point on the  $x$  axis around which a simulated swiveling 'leading wheel' is rotating. Using the non-holonomic constraint equation for this leading wheel one can derive the differential equation of first order in time for the linear behaviour of the lateral force generation of the wheel (see Appendix 2). Today this differential

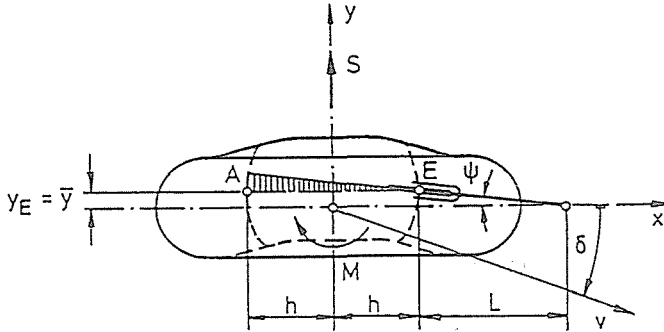


Fig. 3. Rolling lateral elastic wheel: moving plane  $x, y$ , contact length  $2h$ , cornering force  $S$ , cornering moment  $M$ , cornering angle  $\delta$ , swiveling angle  $\psi$ , lateral global deformation  $\bar{y}$ , entrance  $E$ , outlet  $A$ , local deformation at  $A$  is  $2h\psi$ , relocation length is  $L$ , simple model, load slowly changing.

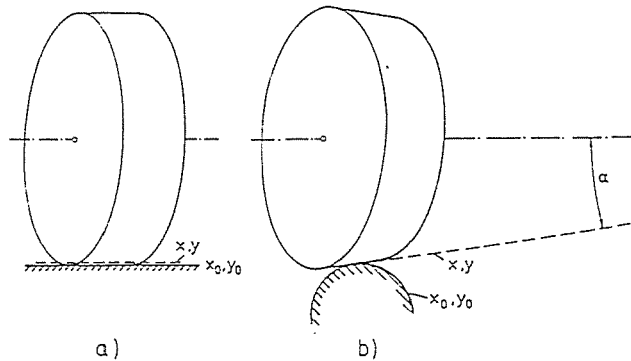


Fig. 4. Two surfaces which can be flattened without deformation: a small penetration of two elastic bodies produces small tangential deformation and can be added to the relative motion of the two planes, cone angle produces spin.

equation is generally used in industry. It can be used also for longitudinal forces by aid of a shorter relaxation length.

There are three statements which need to improve this equation:

1. The area of contact has a deformation field perhaps with short wavelength which is only poor approximated by linear increasing deformation with contact length.
2. The real pressure distribution does not allow tangential forces bigger than the friction limit.
3. Non-smooth surfaces need a discontinuous theory.

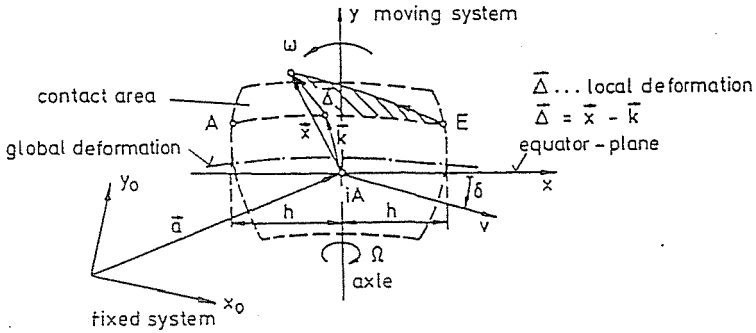


Fig. 5. Rolling elastic wheel: global deformation  $k$ , local deformation  $\Delta$ , fast changing contact area  $h = h(t)$ , fast changing of  $\delta(t)$ ,  $v(t)$ ,  $\omega(t)$  and load, complex model

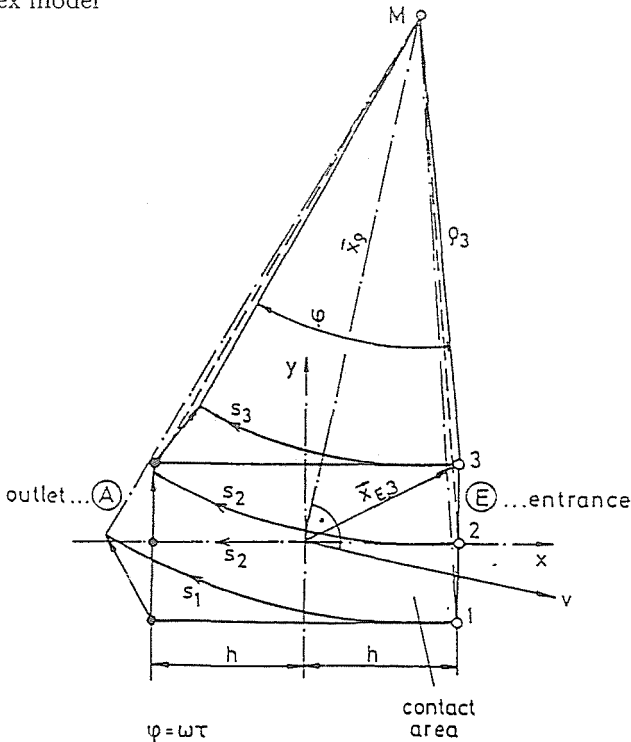


Fig. 6. Stationary rolling of a deformable cylindrical surface: local deformations when the equator line (2) has no longitudinal slip

## 2. Non-Holonomic Rolling Condition for 2-Dimensional Contact

We begin with the first statement. The non-holonomic rolling condition in this contact area can now be formulated by the idea that we have two

reference planes which are moving one on another. The basic plane  $x_0, y_0$  is the road and the moving plane  $x, y$  is oriented by the intersection line of the wheel plane with the road plane. On this line is laying the idealized contact point i.A, which is the intersection of the steepest descent line with the road plane.

Looking for bodies and surfaces with small deformation in normal contact we find only a cylinder on a horizontal plane rolling with horizontal axis or a cone on a cylinder, *Fig. 4*. For both cases there exists in the surface  $x_0, y_0$  there exists a point  $M$  around that point the wheel is turning. So we can use this simplified geometry to define the real contact in case of very small deformations. A small flattening of the wheel can be used to define very small tangential deformations  $u(x, y)$  and  $v(x, y)$  in the moving plane  $x, y$ . We distinguish between small, 'local' deformations  $\Delta_x(x, y), \Delta_y(x, y)$  and 'global' deformations (for instance lateral bending or eigenmodes) of the wheel  $k_x(x, y)$  and  $k_y(x, y)$ , see *Fig. 5*.

$$\begin{aligned} u(x, y) &= k_x(x, y) + \Delta_x(x, y), \\ v(x, y) &= k_y(x, y) + \Delta_y(x, y). \end{aligned}$$

The area of contact must be known from a contact theory or from measurements, also the functions  $\mathbf{k}$  and  $\Delta$

Because of the fact that the two planes have a common point  $M$  which is not moving in both planes we can formulate the non-holonomic rolling condition:

$$e_\rho(\mathbf{x}) \cdot d\mathbf{x} = 0.$$

At first we look for the movement of a contact point in the plane  $x, y$  when it is *fixed* in the plane  $x_0, y_0$ , see *Fig. 5*:

$$\mathbf{x}_0 = \mathbf{a} + \mathbf{x} = \text{const!}$$

In the moving system  $x, y$  we get by aid of the Euler equation:

$$\mathbf{v} + \mathbf{x} + \omega \mathbf{x} \times \mathbf{x} = \mathbf{0}.$$

From this we get the differential equation:

$$(*) \quad \boxed{\dot{\mathbf{x}} = \mathbf{A}\mathbf{x} + \mathbf{f}}$$

the matrix  $\mathbf{A}$  and vectors  $\mathbf{f}, \mathbf{x}$  are

$$\mathbf{A} = \begin{pmatrix} 0 & \omega \\ -\omega & 0 \end{pmatrix}, \quad \mathbf{f} = \begin{Bmatrix} -v \cos \delta \\ v \sin \delta \end{Bmatrix}, \quad \mathbf{x} = \begin{Bmatrix} x \\ y \end{Bmatrix}.$$

If all parameters are constant ( $\omega_0 v_0 \delta_0$ ) the solution consists of circles

$$\mathbf{x}_{(t)} = \mathbf{D}_{(t)}(\mathbf{x}_{(t_1)} - \mathbf{x}_\rho) + \mathbf{x}_\rho,$$

where  $\mathbf{D}_{(t)} = e^{\mathbf{A}_0(t-t_1)}$ ,  $\mathbf{x}_\rho = -\mathbf{A}_0^{-1}\mathbf{f}_0$ . Expanding  $e^{\mathbf{A}_0(t-t_1)}$  one finds:

$$\mathbf{D}(t) = \begin{pmatrix} \cos \varphi & \sin \varphi \\ -\sin \varphi & \cos \varphi \end{pmatrix}, \quad \varphi = \omega_0(t - t_1).$$

This solution produces the following field of relative motions, see *Fig. 6*. If the contact points 1, 2, 3 are touching the ground plane at the same time  $t_1 = t_E$  and defining the running time in contact by  $\tau = t_A - t_E$  the angle  $\varphi$  is for all points 1, 2, 3 the same.

For a differential element of the way of the moving point we get

$$(\mathbf{x} - \mathbf{x}_\rho) \cdot d\mathbf{x} = 0$$

which is a non-holonomic constraint. The location of  $M$  is in every case

$$\mathbf{x}_\rho = \left( \frac{v}{\omega} \sin \delta, \frac{v}{\omega} \cos \delta \right)$$

so one gets the constraint equation:

$$\left( x - \frac{v}{\omega} \sin \delta \right) dx + \left( y - \frac{v}{\omega} \cos \delta \right) dy = 0.$$

Multiplying by  $\omega$ , re-arranging and using the time element  $dt$  leads to

$$\frac{dx}{\omega y - v \cos \delta} = \frac{dy}{\omega x - v \sin \delta} = \frac{dt}{1},$$

which defines a family of characteristics. Defining  $\mathbf{x} \equiv \mathbf{x}^*(x, y, t)$  as a non-stationary field of moving lines of contact points

$$\dot{\mathbf{x}} = \frac{\partial \mathbf{x}}{\partial x} \frac{dx}{dt} + \frac{\partial \mathbf{x}}{\partial y} \cdot \frac{dy}{dt} + \frac{\partial \mathbf{x}}{\partial t}$$

it follows

$$\dot{\mathbf{x}} = \frac{\partial \mathbf{x}}{\partial x} (\omega y - v \cos \delta) + \frac{\partial \mathbf{x}}{\partial y} (\omega x - v \sin \delta) + \frac{\partial \mathbf{x}}{\partial t} = \mathbf{A}\mathbf{x} + \mathbf{f}$$

which are nonlinear because of  $\omega x, \omega y$ . It is important to mention here that numerical integration uses time increments  $\Delta t$  and increments  $\Delta \psi, \delta s_x, \Delta s_y$  defined by

$$\Delta \psi = \omega \Delta t, \quad \Delta s_x = v \cos \delta \Delta t, \quad \Delta s_y = v \sin \delta \Delta t.$$

So we get for the new position of the point  $\mathbf{x}(t + \Delta t) \equiv \mathbf{x}'$  in all cases, even when  $\mathbf{x}_\rho$  goes to infinity (that means pure translation), the following expansions

$$\mathbf{x}' = \mathbf{D}(\mathbf{x} - \mathbf{x}_\rho) + \mathbf{x}_\rho = \mathbf{D}\mathbf{x} + (\mathbf{E} - \mathbf{D})\mathbf{x}_\rho, \quad \text{expanding } \mathbf{D} \text{ to third order :}$$

$$\mathbf{D} \doteq \begin{pmatrix} 1 - \frac{1}{2}\Delta\psi^2, \Delta\psi - \frac{1}{6}\Delta\psi^3 \\ -\Delta\psi + \frac{1}{6}\Delta\psi^3, 1 - \frac{1}{2}\Delta\psi^2 \end{pmatrix}, \quad \mathbf{x}_\rho = \left\{ \begin{array}{l} \Delta s_y / \Delta\psi \\ \Delta s_x / \Delta\psi \end{array} \right\}.$$

$$x' = \left(1 - \frac{1}{2}\Delta\psi^2\right)x + \left(\Delta\psi - \frac{1}{6}\Delta\psi^3\right)y - \left(1 - \frac{1}{6}\Delta s_x + \frac{1}{2}\Delta\psi\Delta s_y\right),$$

$$y' = \left(-\Delta\psi + \frac{1}{6}\Delta\psi^3\right)x + \left(1 - \frac{1}{2}\Delta\psi^2\right)y + \frac{1}{2}\Delta\psi\Delta s_x + \left(1 - \frac{1}{6}\Delta\psi^2\right)\Delta s_y.$$

A transformation which is regular, nevertheless if  $\tan \delta = \frac{\Delta s_y}{\Delta s_x}$  is small or not. The rotation  $\Delta\psi$  must be small, therefore it is necessary to look for the highest frequency of the rolling system with respect to the Shannon theorem (for numerical treatment).

The created tangential forces in the contact area are computed in every timestep using the local deformation vector  $\Delta$ . With these forces one has to compute the dynamics of the global deformations of the wheel and getting the axle forces of the wheel one computes the dynamics of the vehicle masses. So one gets for the next timestep  $v, \delta, \omega$ .

The local deformation vector is in every case an approximation. As it is the difference between  $\mathbf{x}$  and  $\mathbf{k}$  it is an engineering judgement. For instance if we say that the idealized wheel is flattened without deformation (cylinder or cone surface without bending resistance) there is the only global vector for the cases a) and b) of Fig. 4:

$$\text{a) } \mathbf{k} = \begin{Bmatrix} x_E - R\Omega\tau \\ y_E \end{Bmatrix}, \quad \text{b) } \mathbf{k} = \begin{Bmatrix} x_E - R\Omega\tau \\ y_E + \frac{h^2 - x^2}{2\rho} \end{Bmatrix} \quad \begin{array}{l} \tau = \frac{h-x}{v \cos \delta} \\ \rho = \frac{R}{\sin \alpha} \end{array}$$

with  $h \ll \rho$ .

In case of small lateral movement  $y(x, t)$  of the contact points along  $-h \leq x \leq h$ ,  $|\delta| \ll 1$ ,  $|\omega h| \ll 1$  and constant velocity  $v$ , we get the well known equation of B.v. Schlippe, R. Dietrich:

$$\frac{\partial y(x, t)}{\partial x}(-v) + \frac{\partial y(x, t)}{\partial t} = -\omega x + v\delta.$$

This equation was then solved by Smiley using power series in time.

Starting again from first formula (\*) and changing to integral equations one may use a Picard iteration with  $\tau$  as the running time of the point  $x$ :

$$\mathbf{x}_{\nu+1} = \mathbf{x}_E + \int_0^\tau (\mathbf{A}\mathbf{x}_\nu + \mathbf{f}) d\tau,$$

and beginning with straight line running of every point

$$\mathbf{x}_1 = \mathbf{x}_E - \mathbf{e}_x R \Omega \tau \quad \text{with} \quad \tau = \frac{h - x}{v \cos \delta},$$

we find for a cylindrical wheel with small lateral deformation  $y(x, t)$

$$y(x, t) = y_E(t - \tau) + \int_0^\tau (v\delta - \omega x) d\tau$$

a first iteration.

By definition  $d\tau = -\frac{dx}{v_x}$  and  $v_x \doteq v = R\Omega$  (no longitudinal slip) we get the differential form:

$$y(x + dx, t) = y(x, t - d\tau) + (v\delta - \omega x) d\tau.$$

Expanding this to first order

$$y(x, t) + \frac{\partial y}{\partial x} dx = y(x, t) - \frac{\partial y}{\partial t} d\tau + (v\delta - \omega x) d\tau,$$

dropping  $d\tau$ :

$$\frac{\partial y}{\partial t} - v_x \frac{\partial y}{\partial x} = v\delta - \omega x$$

which shows, that this type of equation is only a first approximation.

### 3. Dynamics of Real Wheels Using Continuum Theorie

For technical applications the contact points are not only sticking on the surface of contact they are also slipping when the friction limit for a given pressure distribution is reached. To simplify the model in these cases the velocity of sliding is computed only using the rotation velocity and vibrational velocities of the eigenmodes of the wheel. The local deformation velocity is neglected. So only low frequency self excited excitation is possible. Because of decrease of the friction function with increasing sliding velocity a dynamic rolling stability problem arises: stiction forces and friction forces are nonconservative and so there is a need to get energy losses into the wheel body to stabilize the fast rolling system.

Looking through a running glass plate for the contact behaviour of the points is contact area, see *Fig. 7*, and estimating the moving of white points which are labelled on the surface of the tire and using image processing for instance fir a rolling situation of five degrees of slip angle one sees, see *Fig. 8* that in front of the contact area the points are sticking and later on they are slipping. This behaviour was also computed, see *Fig. 9*, using two lateral

eigenmodes of the wheel, local shear deformation behaviour of the profile elements and given pressure distribution. The area of contact is assumed to be a section of the toroidal shaped tire surface. To increase rolling stability the eigenmodes must be damped.

Finding by resonance excitation for the first two lateral eigenmodes of the tire where the damping is placed, it was found that it is mostly damped in the sidewalls, which can be shown by thermography, see *Fig. 10*. Also the friction behaviour of the profile elements produce damping, which was computed and controlled also by thermography, see *Figs. 11* and *12* and the computed tire forces are also controlled by sinusoidal excitation of the steering angle running the tire on a drum. Reaching the flutter point of the tire at a wavelength of one meter there is shown a ninety degree phase lag in the *Fig. 13*.

Longitudinal and lateral oscillations with higher frequency of the profile elements were introduced into the system by OERTEL who has shown the influence of friction oscillation of the profiles on the generated tangential contact forces (increasing roughness).

#### 4. Dynamics of Rolling Wheels with Non-Smooth Surface

A further discretisation of the whole wheel and of the contact elements was made using particle dynamics. So it was possible to compute simultaneously global deformations, local deformations, pressure forces, see *Fig. 14* and *15*, and friction forces. A non-holonomic constraint equation is not used. There is only used a holonomic constraint equation when a particle is touching the ground. It is assumed that it is sticking in the first time step when touching the ground because there is no tangential local deformation. In the next time step it is proved if it is sliding or not. Naturally one has a high frequency system of particles and one has to use a very short time step for integration.

Lastly the footprint of the tire was computed, see *Fig. 16*, and it was compared with thermographic estimated footprint see *Fig. 17*. So we end with this research, looking for the high-frequency behaviour in contact area up to 2000 Hz, producing solutions and measurements of this behaviour but do not use non-holonomic constraints again, which was done at a first attempt as a good working hypothesis, and later on looking for nonsmooth surfaces the practicability was bad. Going into the details of the profile deformation discretization is always necessary, but we have to be aware of the fact that we lose a possibility of analytical treatment. But otherwise, to understand all phenomena which occur in the contact region, it is necessary to develop complex numerical models for the behaviour of rolling wheels.

Continental 195/65 R 15 Super Contact  
 Cornering Angle  $5^\circ$ , Camber Angle  $0^\circ$ , Vertical Load 4000 N,  
 2.0 bar

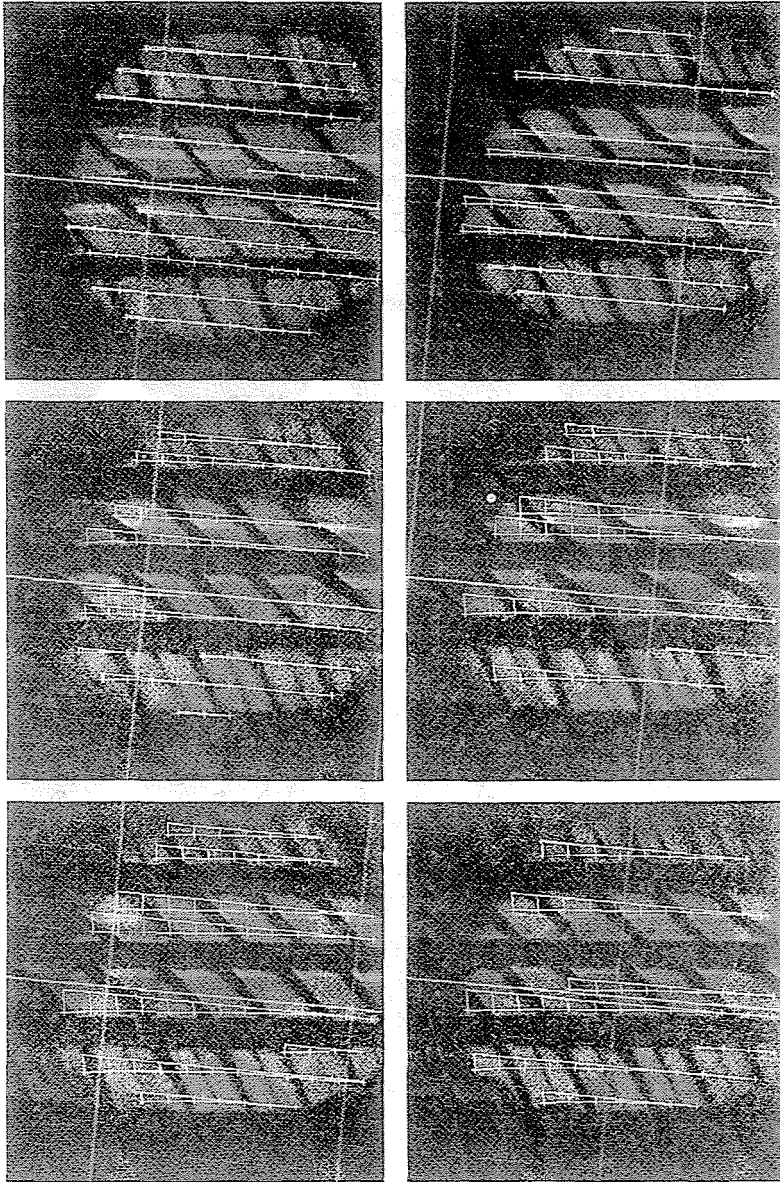


*Fig. 7.* Tire rolling nonstationary on a glass-plate beginning from upper left to right down : white marked points on the profile elements show the movement relative to inclined motion ( $\delta = 5^\circ$ ) of the plate. At the entrance the points move with the same angle, then they slide laterally, velocity is  $v = 2.5$  cm/s.

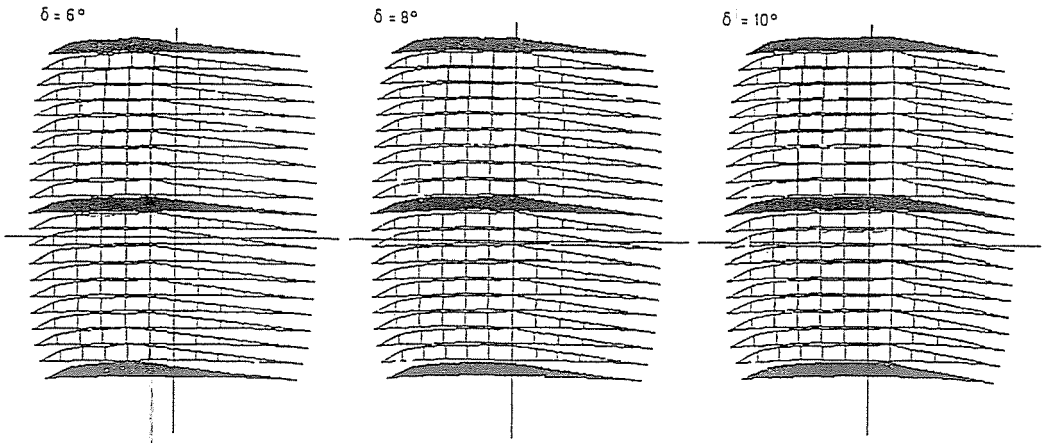


Fig. 8. Computation of rolling situation with  $\delta = 6^\circ, 8^\circ, 10^\circ$  using 21 lines and 13 collocation points on every line

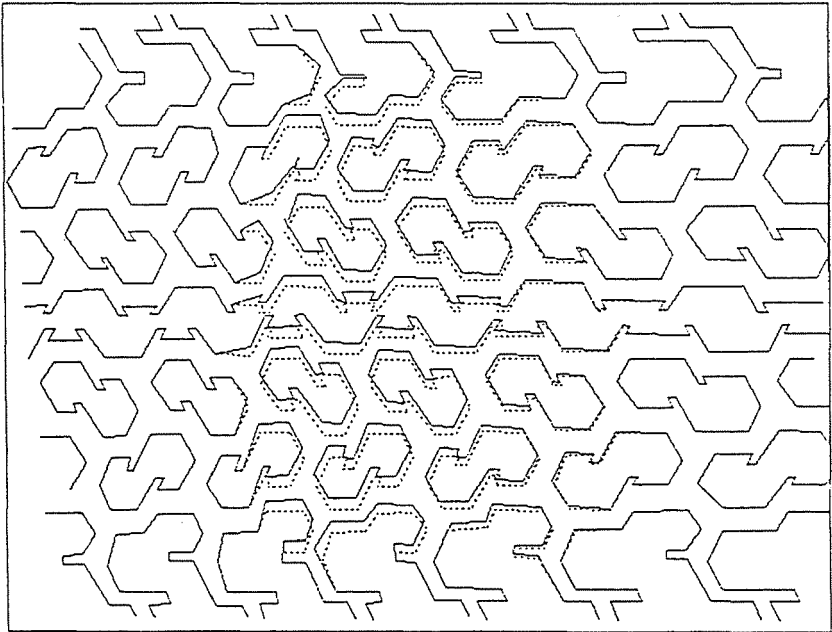


Fig. 9. Local deformation computed for  $\delta = 5^\circ$

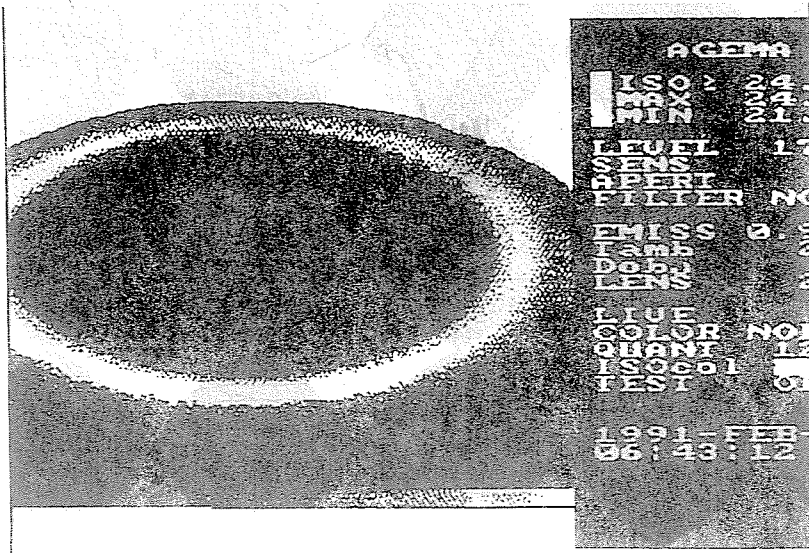


Fig. 10. Eigenmode  $n = 0$  for lateral excitation of the tire

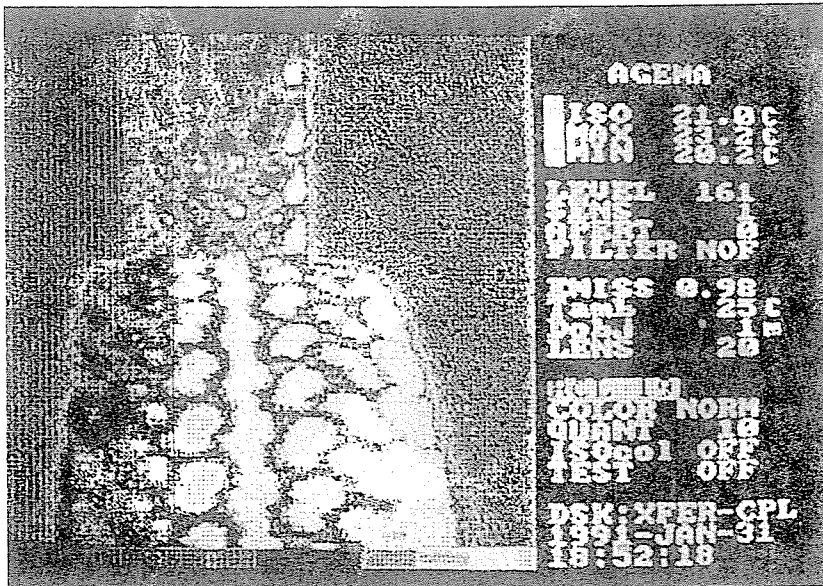


Fig. 11. Thermography of frictional heat up of the slipping profile elements, concerning angle  $5^\circ$ , camber angle  $5^\circ$ , vertical load 3000 N

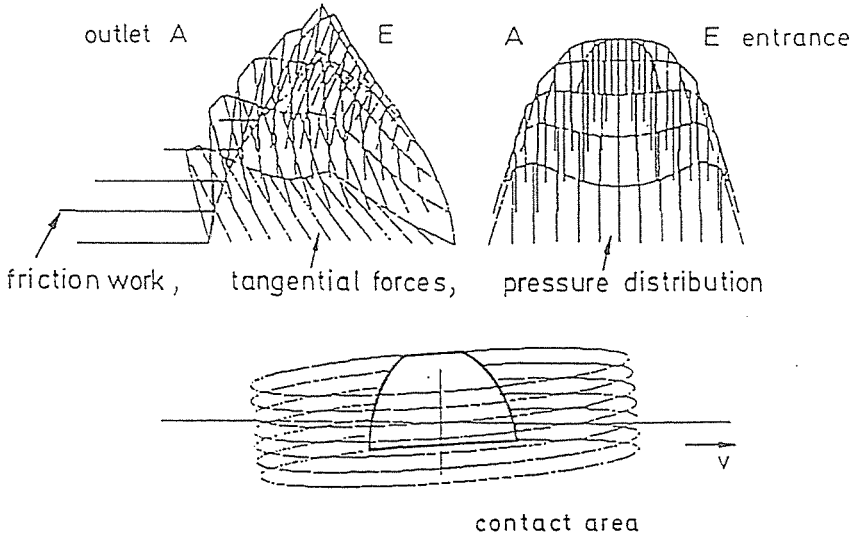


Fig. 12. Computed results of friction work, tangential forces and pressure distribution, stationary rolling

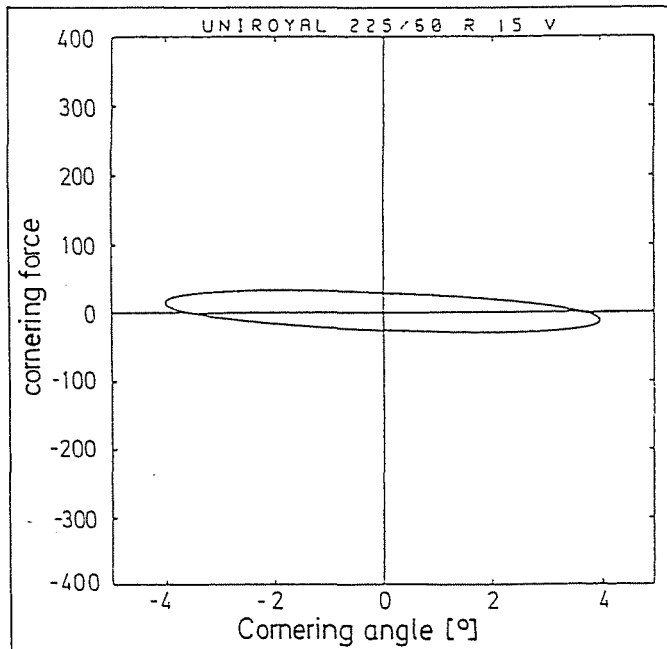


Fig. 13. Computed flutter point for a 225/60 R 15 V tire

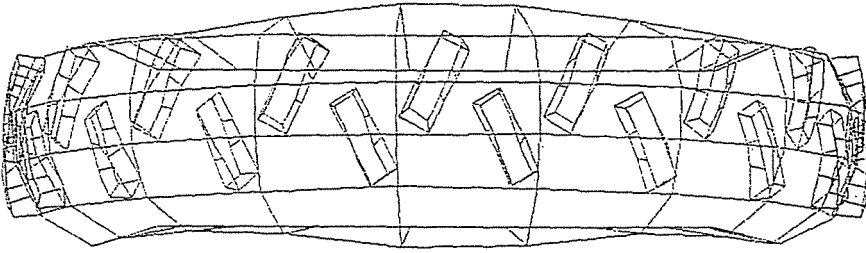


Fig. 14. Computed deformation of a tire model with profile elements, cornering angle  $5^\circ$ , load 3000 N

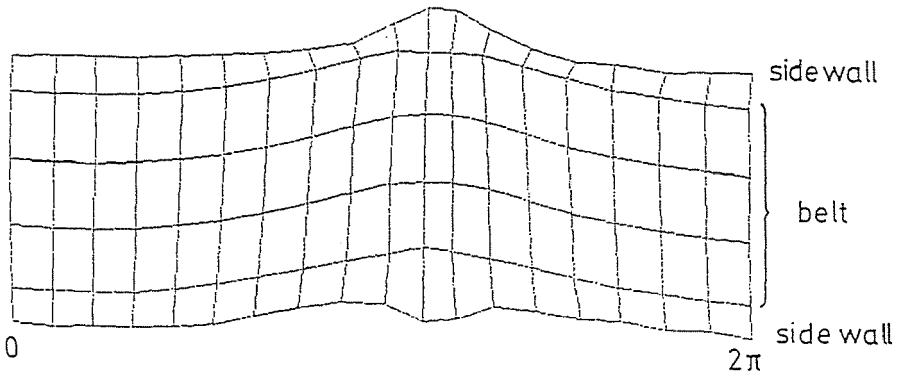


Fig. 15. Computed lateral deformation of the tire carcass

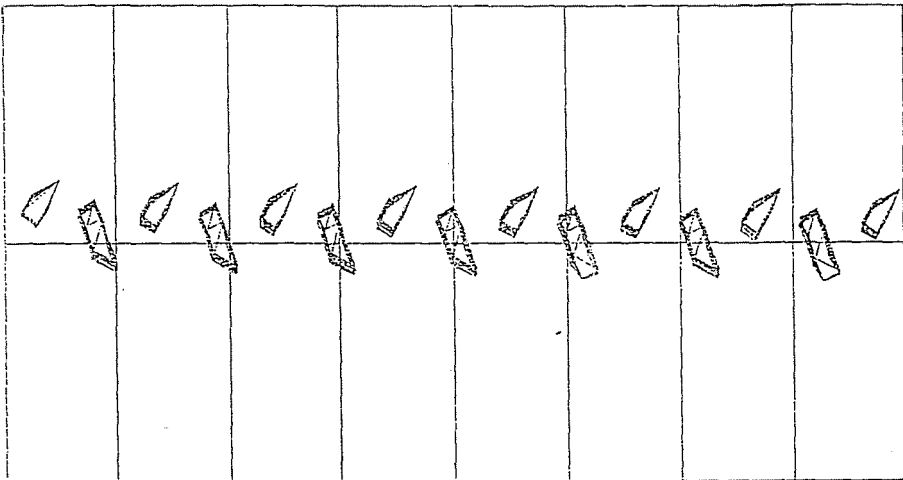


Fig. 16. Computed footprint of model on a plate

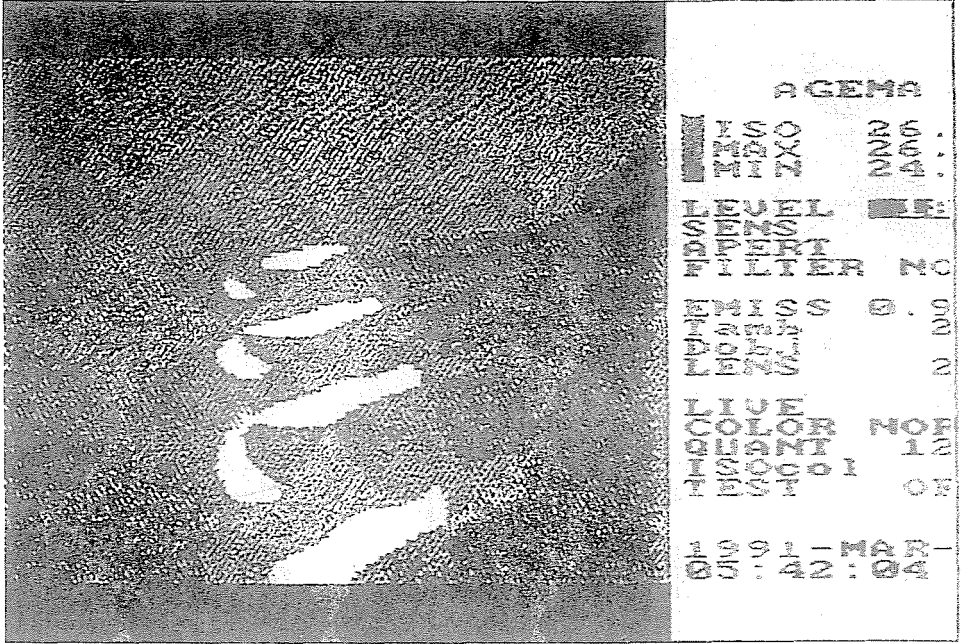


Fig. 17. Thermography of a rolling tire with this profile on a flat bed test rig. cornering angle  $5^\circ$

### Conclusion

The concept of a non-holonomic condition for a single contact point was the first step into dynamics of vehicles. The next step was to extend the concept to a contact line and to a contact area.

Introducing a friction law big problems arise: there is no theory for friction oscillations in continuum theory. But for discrete systems it was possible to produce correct and stable numerical solutions. So it was shown that high frequency behaviour of rolling wheels always needs an engineering decision what eigenmodes have to be used.

Rolling and slipping of real wheels can only be simulated numerically using particle dynamics. Computing the contact of the surface particles touching the ground, it is necessary to use holonomic constraints. The frequency range of the solution is limited to avoid excessive computing time.

### Appendix 1

$$\begin{aligned} m(\dot{v}_x - \omega v_y - \omega^2 a) &= 0, \\ m(\dot{v}_y + \omega v_x + \dot{\omega} a) &= R, \\ I_s \dot{\omega} &= -Ra, \end{aligned}$$

$$0 < v_x = \text{const.}, \quad v_y = \dot{v}_y = 0, \quad \dot{\psi} = \omega,$$

$$m(\omega v_x + \dot{\omega} a) = -I_s \frac{\dot{\omega}}{a},$$

$$\boxed{\dot{\omega} + y\omega = 0}, \quad \lambda = \frac{mav_x}{I_s + ma^2},$$

$$\left\{ \begin{array}{l} \text{stable :} \quad a > 0 \\ \text{unstable :} \quad a < 0 \end{array} \right\} \text{ solution } \omega = \omega_0 e^{\lambda t}$$

### Appendix 2

$$\mathbf{v}_E = \left\{ \begin{array}{l} v \\ -v\delta + h\omega \end{array} \right\} + \left\{ \begin{array}{l} 0 \\ \dot{\psi}L \end{array} \right\} + \left\{ \begin{array}{l} -v \\ v\psi \end{array} \right\} \stackrel{!}{=} \mathbf{0}$$

$$\rightarrow v\psi + h\omega + L\dot{\psi} - v\delta = 0$$

$$\psi = \frac{yE}{L}, \quad h\omega \approx 0 \quad \left( h \ll \rho = \frac{v}{\omega} \right),$$

$$\dot{y}_E + v \left( \frac{\dot{y}_E}{L} - \delta \right) = 0, \quad c_S y_E = S,$$

$$S = c_S L \left( \delta - \frac{\dot{y}_E}{v} \right) = c_S L \rho_{\text{eff.}}$$

$c_S L$  ... cornering stiffness,

$$M \doteq \frac{1}{3} hS \quad (\text{linear distribution})$$

### References

- [1] BÖHM, F.: Theorie schnell veränderlicher Rollzustände für Gürtelreifen, *Ingenieur-Archiv*, Vol. 55 (1985) pp. 30-44.
- [2] BÖHM, F.: Einfluß der Laufflächeneigenschaften von Gürtelreifen auf den instationären Rollzustand, DKG-Tagung, Mai 1987 in Wien (Österreich).
- [3] KMOCH, K.: Meßtechnische Methoden zur Bewertung dynamischer Reifeneigenschaften, Dis. 1992, TU Berlin.
- [4] OERTEL, C.: Untersuchung von Stick-Slip-Effekten am Gürtelreifen, Dis. 1990, TU Berlin.